Dynamic stability of Małgosia II aircraft with use of MSC.Adams

P. Wiśniowski, T. Uhl, E. Margański
Department of Robotics and Mechatronicks
AGH University of Science and Technology
Kraków, Polnad

1. Abstract

This paper deals with dynamic stability analysis of Małgosia II aircraft. Results from MSC.Nastran which was used to calculate aerodynamic coefficients were taken as input data in order of building multi-body model of aircraft in MSC.Adams.

Presented method of calculation dynamic response of aircraft in time domain can be used to easily check dynamic stability and also include effects of pilot input.

The calculated results will also be presented.

2. Introduction

Małgosia II is a prototype of light, propeller driven, two person plane with rare wings configuration of canard type designed by Edward Margański. This airplane configuration will be used to present the analysis methodology.

The speed of aircraft ranges from 160 to 220 km/h. The reference wing area is equal to 11,42m^2, the reference wing span is 8,967m , and mean aerodynamic chord is equal to 1,513m. The empty weight is 475 kg and maximal take of weight is 794 kg.

The NACA641412 is used as main wing profile and FX71-L-150 for a front wing profile.

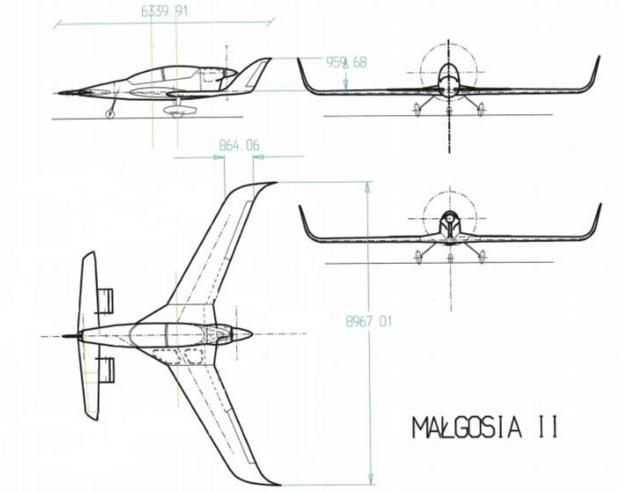

Fig. 1 Views of Małgosia II aircraft

The paper is organized as follows. Section 3 describes goal of this paper. Section 4 contains introduction and basic data concerning multi-body model. Section 5 defines equations of aerodynamic force acting on aircraft. Section 6 describes how the propeller was modeled. Section 7 lists analyzed cases and section 8 presents the results. Finally, section 9 presents our conclusions.

3. Goal of the paper

The goal of this paper is to prove that analyzed plane is dynamically stable and can be controlled by pilot. Additionally effectiveness of all control surfaces will be calculated.

4. MSC.Adams model

MSC.Adams model consists seven rigid bodies connected by revolute joints. This bodies include main plane body and separate control surface bodies:

- Left Aileron
- Right Aileron
- Left Rudder
- Right Rudder
- Horizontal stabilizer
- Horizontal stabilizer trim tabs

The deflection of horizontal stabilizer trim tabs is connected by coupler with horizontal stabilizer deflection. The ratio between this deflections is 1 to 14.

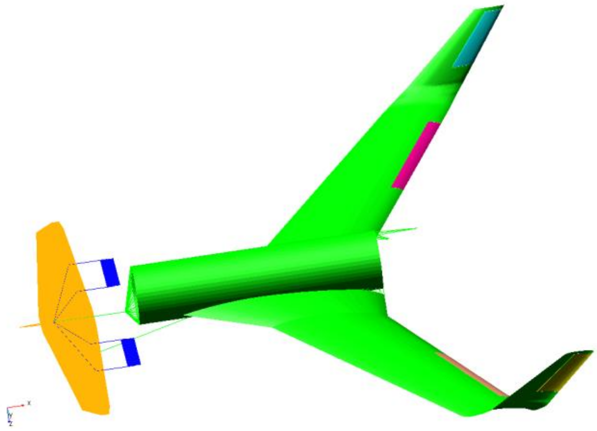

Fig. 2 MSC.Adams model of Malgosia II aircraft.

Main coordinate system which is used for most measures and calculating aerodynamic force is bounded with main plane body and its origin is defined at c.g. of aircraft. X- axis is defined backward and Z-axis downward.

Measures needed for calculating aerodynamic force include:

- v_x - longitudinal speed of main plane body (typically negative as plane flies forward),
- v_y - side speed of main plane body,
- v_z - vertical speed of main plane body,
- ω_x - roll speed of main plane body,
- ω_y - pitch speed of main plane body,
- ω_z - yaw speed of main plane body,
- $\alpha = arctan(\frac{-v_z}{-v_x})$- angle of attack,
- $\beta = arctan(\frac{v_y}{-v_x})$- side angle,
- P - dynamic pressure,

Pilot control input data:

- δ_c – horizontal stabilizer deflection,
- δ_{cr} – horizontal stabilizer trim tabs deflection,
- δ_{al} – left aileron deflection,
- δ_{ar} – right aileron deflection,
- δ_{rl} – left rudder deflection,
- δ_{rr} – right rudder deflection.

Dynamic pressure is calculated as:

$$P = 0.5\,\rho\,(v_x^2 + v_y^2 + v_z^2) \tag{1}$$

$\rho = 1.168\ kg/m^3$ - air density.

5. Aerodynamic force

The aerodynamics is computed by the use of Double-Lattice subsonic lifting surface theory (DLM) implemented in MSC.Nastran in which the linearized potential flow theory is used to compute aerodynamic coefficients listed below.

Table 1 Calculated stability derivative coefficients

[-]	T_y	T_z	M_x	M_y	M_z
Reference (ref)	-4.7439 10^{-5}	-6.0673 10^{-1}	-8.6856 10^{-5}	6.2013 10^{-1}	-1.6776 10^{-5}
Angle of attack (α)	-6.5422 10^{-4}	6.7201 10^{0}	2.0096 10^{-4}	-5.8595 10^{-1}	-1.1490 10^{-4}
Side angle (β)	-3.9917 10^{-1}	5.7287 10^{-4}	-1.2385 10^{-1}	-5.9399 10^{-4}	-7.5223 10^{-2}
Roll speed (ω_x)	-3.6376 10^{-1}	-3.9477 10^{-4}	-7.2210 10^{-1}	2.6992 10^{-4}	-9.3628 10^{-2}
Pitch speed (ω_y)	-1.4106 10^{-3}	7.9096 10^{0}	3.5664 10^{-4}	-1.6095 10^{+1}	-2.5898 10^{-4}
Yaw speed (ω_z)	-2.0183 10^{-1}	2.6154 10^{-4}	-7.0454 10^{-2}	-2.8057 10^{-4}	-5.0920 10^{-2}
Horizontal stabilizer (δ_c)	-2.6438 10^{-5}	6.4380 10^{-1}	7.2125 10^{-6}	2.3177 10^{0}	-4.6842 10^{-6}
Trim tabs (δ_{cr})	-4.2885 10^{-6}	7.6683 10^{-2}	1.1813 10^{-6}	3.2809 10^{-1}	-7.5896 10^{-7}
Left aileron (δ_{al})	2.2503 10^{-2}	3.9074 10^{-1}	1.1870 10^{-1}	-3.8042 10^{-1}	5.7978 10^{-3}
Right aileron (δ_{ar})	2.2592 10^{-2}	-3.9070 10^{-1}	1.1868 10^{-1}	3.8040 10^{-1}	5.8147 10^{-3}
Left rudder (δ_{rl})	7.0520 10^{-2}	4.0482 10^{-2}	2.1685 10^{-2}	-5.7623 10^{-2}	1.9824 10^{-2}
Right rudder (δ_{rr})	7.0485 10^{-2}	-4.0523 10^{-2}	2.1703 10^{-2}	5.7678 10^{-2}	1.9815 10^{-2}

Aerodynamic force is modeled as generative force acting on c.g. of airplane. The force has 3 force components and 3 torque components. Due to lack of possibility of calculating drag coefficients by using DLM the longitudinal force will be discussed later.

$$F_y = P\,S\,(c_{Ty\,ref} + c_{Ty\,\alpha}\,\alpha + c_{Ty\,\beta}\,\beta + (c_{Ty\,\omega x}\,\omega_x B + c_{Ty\,\omega y}\,\omega_y C + c_{Ty\,\omega z}\,\omega_z B)/2v + c_{Ty\,\delta c}\,\delta_c + c_{Ty\,\delta cr}\,\delta_{cr} + c_{Ty\,\delta al}\,\delta_{al} + c_{Ty\,\delta ar}\,\delta_{ar} + c_{Ty\,\delta rl}\,\delta_{rl} + c_{Ty\,\delta rr}\,\delta_{rr}) \tag{2}$$

$$F_z = P\,S\,(c_{Tz\,ref} + c_{Tz\,\alpha}\,\alpha + c_{Tz\,\beta}\,\beta + (c_{Tz\,\omega x}\,\omega_x B + c_{Tz\,\omega y}\,\omega_y C + c_{Tz\,\omega z}\,\omega_z B)/2v + c_{Tz\,\delta c}\,\delta_c + c_{Tz\,\delta cr}\,\delta_{cr} + c_{Tz\,\delta al}\,\delta_{al} + c_{Tz\,\delta ar}\,\delta_{ar} + c_{Tz\,\delta rl}\,\delta_{rl} + c_{Tz\,\delta rr}\,\delta_{rr}) \tag{3}$$

$$M_x = P\,S\,B\,(c_{Mx\,ref} + c_{Mx\,\alpha}\,\alpha + c_{Mx\,\beta}\,\beta + (c_{Mx\,\omega x}\,\omega_x B + c_{Mx\,\omega y}\,\omega_y C + c_{Mx\,\omega z}\,\omega_z B)/2v + c_{Mx\,\delta c}\,\delta_c + c_{Mx\,\delta cr}\,\delta_{cr} + c_{Mx\,\delta al}\,\delta_{al} + c_{Mx\,\delta ar}\,\delta_{ar} + c_{Mx\,\delta rl}\,\delta_{rl} + c_{Mx\,\delta rr}\,\delta_{rr}) \tag{4}$$

$$M_y = P\,S\,C\,(c_{My\,ref} + c_{My\,\alpha}\,\alpha + c_{My\,\beta}\,\beta + (c_{My\,\omega x}\,\omega_x B + c_{My\,\omega y}\,\omega_y C + c_{My\,\omega z}\,\omega_z B)/2v + c_{My\,\delta c}\,\delta_c + c_{My\,\delta cr}\,\delta_{cr} + c_{My\,\delta al}\,\delta_{al} + c_{My\,\delta ar}\,\delta_{ar} + c_{My\,\delta rl}\,\delta_{rl} + c_{My\,\delta rr}\,\delta_{rr}) \tag{5}$$

$$M_z = P\,S\,B\,(c_{Mz\,ref} + c_{Mz\,\alpha}\,\alpha + c_{Mz\,\beta}\,\beta + (c_{Mz\,\omega x}\,\omega_x B + c_{Mz\,\omega y}\,\omega_y C + c_{Mz\,\omega z}\,\omega_z B)/2v + c_{Mz\,\delta c}\,\delta_c + c_{Mz\,\delta cr}\,\delta_{cr} + c_{Mz\,\delta al}\,\delta_{al} + c_{Mz\,\delta ar}\,\delta_{ar} + c_{Mz\,\delta rl}\,\delta_{rl} + c_{Mz\,\delta rr}\,\delta_{rr}) \tag{6}$$

$S = 11.42\ m^2$ – wings reference area,
$B = 8.967\ m$ – wings reference span,
$C = 1.513\ m$ – wings reference chord,

$c_{i\,j}$ – stability aerodynamic coefficient taken from appropriate i column and j row from Table 1.

An assumption was made in order of computing the longitudinal drag force: the aerodynamic drag force at normal course with 190 km/h is equal to trust force generated by 70HP engine with 80% propeller efficiency.

The drag coefficient is calculated as follows:

$$c_{Tx\,ref} = \frac{W_{engine}\,\mu_{prop}}{0.5\,\rho\,\mathrm{v}_{Tx\,ref}^3\,S} = 0.042 \tag{7}$$

$W_{engine} = 51.484\ kW$ – engine power,
$\mu_{prop} = 0.80$ – propeller efficiency,
$v_{x\,ref} = 190\ km/h$ - reference speed.

In this way longitudinal aerodynamic force is defined as (note that effects of increasing drag force due to control surface deflections are neglected as less important):

$$F_x = S\,P\,c_{Tx\,ref} \tag{8}$$

6. Propeller influence

The propeller is modeled as trust force and rolling torque.

The trust force is defined as:

$$F_{prop} = \frac{W_{engine}\,\mu_{prop}\,\delta_{trust}}{v_x} \tag{9}$$

δ_{trust} – pilots control of engine power (note that if $\delta_{trust} = 1.0$ the engine generates nominal power).

The torque generated by propeller is defined as:

$$M_{x\,prop} = \frac{W_{engine}\,\delta_{trust}}{\omega_{prop}} \tag{10}$$

$\omega_{prop} = 50\,000\ rpm$ – propeller's rotational speed (note that constant-speed propeller was assumed).

The effect of propeller on directional stability is neglected as less important.

7. Analyzed cases

All analyzed scenarios are fully described by defined time history of pilot inputs and initial conditions. Initial conditions include initial velocities and initial position of c.g. For some simplification only initial longitudinal velocity (v_{x0}) is defined and all other initial conditions are taken as zeroes.

The non-zeroes values of control surface deflections are results from MSC.Nastran solution and are required for obtaining straight fly.

Table 2 Analyzed cases.

Id.	Description	δ_c	δ_{cr}	δ_{al} and δ_{ar}	δ_{rl} and δ_{rr}	δ_{trust}	v_{x0}
		[deg]	[deg]	[deg]	[deg]	[-]	[km/h]
LC1	Straight fly	-0.02	0.00	0.00	0.00	1.00	-190.0
LC2	Minimum speed fly	-0.03	0.00	-0.01	0.00	0.71	-160.0
LC3	Maximum speed fly	-0.02	0.00	0.00	0.00	1.34	-220.0
LC4	Angle of attack disturbance	-0.02	0.00	0.00	0.00	1.00	-190.0
LC5	Side angle disturbance	-0.02	0.00	0.00	0.00	1.00	-190.0
LC6	Canard deflection	1.00	-0.07	0.00	0.00	1.00	-190.0
LC7	Aileron deflection	-0.02	0.00	5.00	0.00	1.00	-190.0
LC8	Rudder deflection	-0.02	0.00	0.00	5.00	1.00	-190.0

For cases 4 and 5 the α and β additional angle disturbances are defined as smooth step function:

$$\delta_{dist} = f(t, 9s, 10deg, 10s, 0deg) \tag{11}$$

t – time,
$f()$ – MSC.Adams smooth step function.

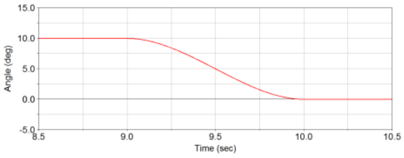

Fig. 3 MSC.Adams smooth step function f(t ,9s ,10deg ,10s ,0deg).

8. Results

Longitudinal stability

The subject of study of first four load cases is longitudinal dynamic stability. This topic mainly focuses on exchanging energy between kinetic energy and potential energy of aircraft.

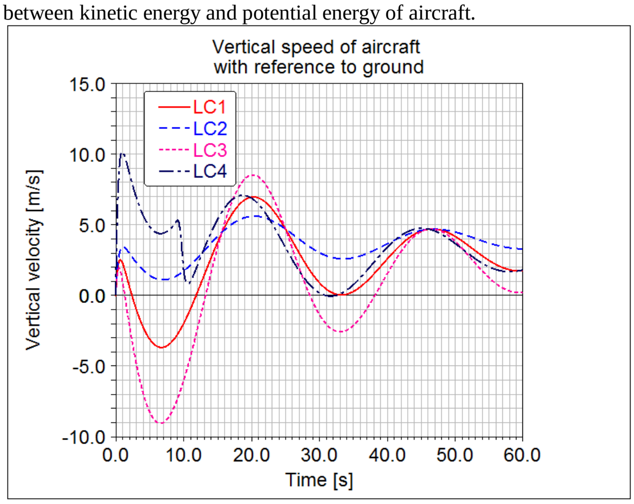

Fig. 4 Vertical speed of aircraft during longitudinal stability load cases.

On Fig. 4 some damped oscillations can be seen as a result of changing altitude of aircraft. The period of this oscillations is 25.6 s so the pilot can manually correct them. This is the aircraft's phugoid mode.

The amplitude of this oscillations is decreasing which is dynamic stability condition. The calculated damping for this mode is 13.7% of critical damping.

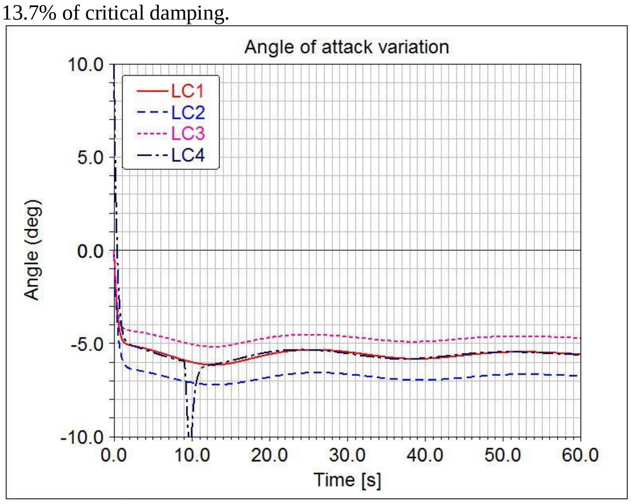

Fig. 5 Angle of attack during longitudinal stability load cases.

The calculated angle of attack tends to be a constant value depending mainly on speed of aircraft. Also it can be clearly seen that after additional disturbance aircraft tends to align its course direction with the wind direction without any oscillations (this mode is critically damped). This implies that the aircraft is dynamically stable after vertical wind gusts.

Directional and lateral stability coupling

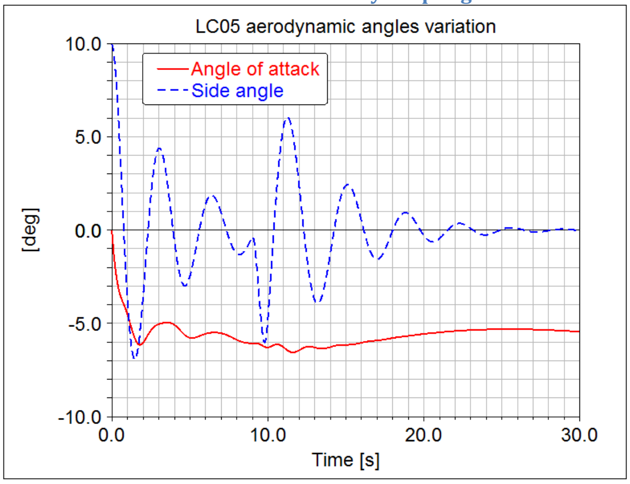

Fig. 6 Aerodynamic angles variation during LC5 scenario.

The aircraft after side wind gusts tends to align its course with the wind direction with some damped oscillations. It corrects its course both by roll and yaw motions. Strong coupling can be seen between this two degrees of freedom of aircraft.

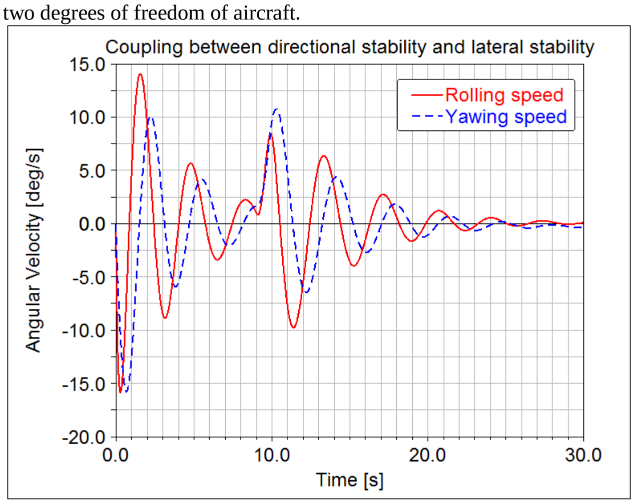

Fig. 7 Rolling and yawing speed after side wind gust.

After this disturbance aircraft first tends to roll in order of getting the wind direction under the wings and then vertical surfaces start to work by correcting the course. This mode is known as Dutch roll mode.

The frequency of this oscillations is 0.267 Hz and damping is 14.1%. The aircraft is dynamically stable after side wind gusts.

Control surface effectiveness

The aim of LC6, LC7 and LC8 is to study control surface effectiveness. Each control surface have primary impact on appropriate motion of aircraft and results in creating torque. Rolling, pitching and yawing motion also creates damping torque which limits the effectiveness of control surface.

The pitching speed plotted on Fig. 8 remains constant with no oscillations as the aircraft is heavily damped during this motion as a result of high distance between c.g. of aircraft and aerodynamic center of horizontal stabilizer.

The rolling speed increases slowly with time as a result of increasing aircrafts speed during nosedive which is a result of this maneuver. Only the initial rolling speed is taken under consideration during calculation of aileron effectiveness.

The yawing speed results are similar to those obtained for LC5 as both of them effect in disturbance in side angle. The difference is during yawing with rudder deflection constant yawing speed is obtained. Also after around 2 s negative yawing speed was obtained which can be problematic for pilot as it is not desired behavior of aircraft.

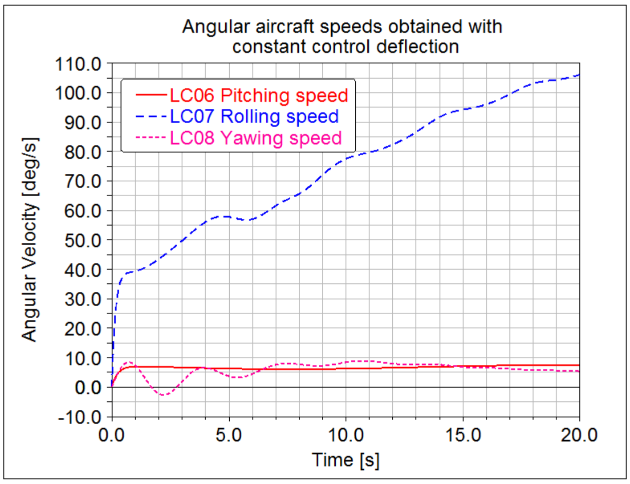

Fig. 8 Angular aircraft speeds obtained with constant control deflection.

The control surface effectiveness coefficients are calculated as:

$$\varepsilon_a = \frac{\omega_{x\,LC7}\ B}{2v\ (\delta_{al} + \delta_{ar})} = 0.319 \tag{12}$$

$$\varepsilon_c = \frac{\omega_{y\,LC6}\ C}{2v\ \delta_c} = 0.099 \tag{13}$$

$$\varepsilon_r = \frac{\omega_{z\,LC8}\ B}{2v\ (\delta_{rl} + \delta_{rr})} = 0.072 \tag{14}$$

$\omega_{x\,LC7} = 37.50\ deg/s$ – initial rolling speed of aircraft after ailerons deflection,

$\omega_{y\,LC6} = 6.90\ deg/s$ – pitching speed of aircraft after horizontal stabilizer deflection,

$\omega_{z\,LC8} = 8.45\ deg/s$ – yawing speed of aircraft after rudder deflection.

It can be clearly seen that the aircraft is very sensitive on ailerons input. Also the horizontal stabilizer effectiveness is similar to ruder effectiveness but it lacks of undesired oscillating behavior. It is recommended to use both aileron and horizontal stabilizer control surfaces during turn maneuver as it will not induce oscillations and the effectiveness of maneuver will be similar.

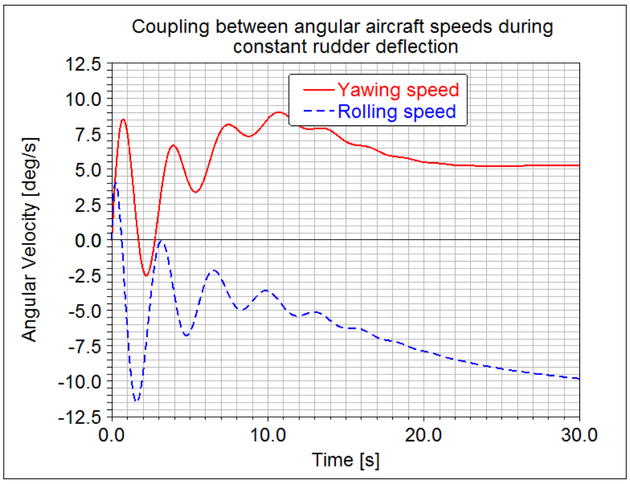

Fig. 9 Coupling between roll and yaw motion of aircraft during constant rudder deflection.

As seen of Fig. 9 rudder can be easily used as secondary rolling control surface as its deflection results both on yawing and rolling of aircraft.

General Małgosia II aircraft modes

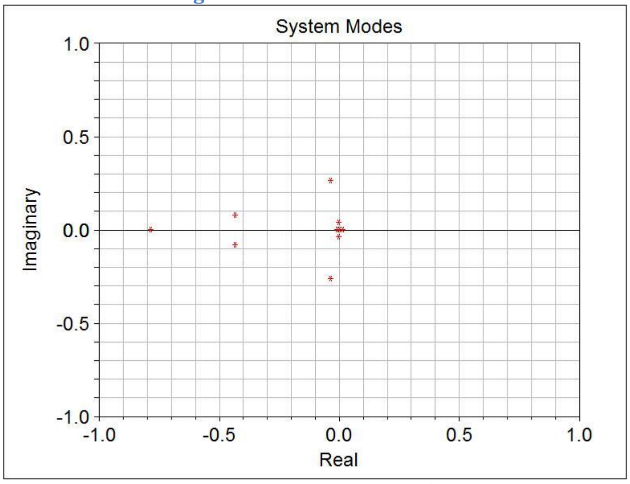

Fig. 10 Calculated linear modes of Malgosia II aircraft.

Linear modes of model at LC1 at time of 15s were calculated with use of MSC.Adams Linear Modes capability.

This results describe whole dynamic behavior of aircraft in short form of frequency, damping and mode shape information.

Table 3 Calculated Linear modes of Małgosia II aircraft.

Mode no.	Frequency Hz	Damping [-]	Re. [-]		Im. [-]
1	0.000	0.000	0.000	+/-	0.000i
2	0.000	0.000	0.000	+/-	0.000i
3	0.000	0.000	0.000	+/-	0.000i
4	0.010	1.000	-0.010	+/-	0.000i
5	0.012	1.000	0.012	+/-	0.000i
6	0.788	1.000	-0.788	+/-	0.000i
7	0.039	0.137	-0.005	+/-	0.039i
8	0.442	0.984	-0.435	+/-	0.080i
9	0.267	0.141	-0.038	+/-	0.264i

First three modes are the rigid body translations. Their frequency is 0.0 Hz as the result of neutral equilibrium. The aircraft can be translated without impact on results.

The fourth mode represents yawing motion mode which is critically dumped with low frequency. This mode is not seen on dynamic behavior of aircraft.

The fifth mode is unstable as it describes turning of aircraft caused by unbalanced rolling moments resulting from propeller torque and non-symmetric placement of c.g. of aircraft. It effects in turning aircraft left and starts to become noticeable after 50s. This can be easily corrected by pilot input.

The sixth mode is pure roll mode. It represents the rolling behavior of aircraft and is critically dumped so no roll oscillations should be seen during straight fly.

The seventh mode is the phugoid mode which was described earlier.

The eighth mode is short period mode with shape similar to phugoid mode. This mode is almost critically dumped which is an requirement of dynamic aircraft stability as it cannot be corrected by pilot input due to short period.

The ninth mode represents Dutch roll mode which was described earlier.

9. Conclusions

The analysis of dynamic model shows that the analyzed aircraft is dynamically stable. Equations of motion were build (with use of stability derivatives) and solved in order to analyze dynamic stability of Małgosia II aircraft. All dynamic modes which represents dynamic behavior of aircraft were obtained.

Presented method of calculation dynamic stability of aircraft can be used to at the earliest step of conceptual design without use of time-consuming CFD calculations and wind tunnel tests.

This calculations can be also used without any serious modifications to include deformable structure of aircraft in which case results will be more accurate.

10. References and bibliography

[1] Albano, E., and Rodden, W.P. A Doublet-Lattice Method for Calculating Lift Distributions on Oscillating Surfaces in Subsonic Flows. 1969.

[2] Giesing, J. P., Kalman, T. P., and Rodden, W. P. Subsoic Stedy and Oscilatory Aerodynamic for Multiple Interfering Wings and Bodies. 1972.

[3] MSC.Nastran. Quick Refference Guide. 2013.

[4] MSC.Nastran. Aeroelastic Analysis User's Guide. 2013.

[5] Giesing, J. P., Kalman, T. P., and Rodden, W. P. Correction Factor Techniques for Improving Aerodynamic Prediction Methods: NASA CR 144967, 1976.

[6] MSC.Nastran. Linear Static Analysis User's Guide. 2013.

[7] airfoiltools. [Online] http://airfoiltools.com/.

[8] Caughey, David A. Introduction to aircraft stability and control. New York : Ithaca, 2011.

[9] Flight Emergency & Advanced Maneuvers Training, Lateral/Directional Stability, 2009.

[10] MSC.Adams Linear. Simplifying equations of motion formulated by MSC.Adams to linear form for accurate studies of stability and vibration

[11] Richard L. LeBoeuf, Ken London, MSC.Adams mode verification for spinning spacecraft with Wire Booms, California, 2004.